Vegetation response to hydrologic and geomorphic factors in an arid region of the Baja California Peninsula

Victor M. Rodríguez-Moreno · Stephen H. Bullock

Received: 5 July 2012 / Accepted: 14 September 2013 / Published online: 28 September 2013 © The Author(s) 2013. This article is published with open access at Springerlink.com

Abstract Remotely sensed imageries were used to analyze the response of desert vegetation to physiographic factors and accumulated precipitation in drier and wetter years within a region of >16,500 km² sampled with 5,000 random pixels of 30 m. Vegetation development was indexed by the annual maximum values for greenness (SAVI) and canopy water content (NDII). Precipitation was interpolated from the 0.25° grid of the Tropical Rainfall Measurement Mission satellite-based estimates, showing a regional average of ~55 mm in the wetter year. The vegetation indices were only weakly related to total precipitation, often in a negative sense. Terrain factors that most often affected the vegetation indices, in multiple regression models, were Topographic Wetness Index, elevation, and slope gradient; these

often had different signs for SAVI and for NDII. Models for NDII on intrusive igneous rocks gave better results than on extrusive igneous rocks. The strongest patterns in vegetation development were the contrast among Pacific coast, Cordillera, and Gulf coast subregions and the generally stronger results for NDII than SAVI.

Keywords Remote sensing · Topographic Wetness Index · SAVI · NDII · TRMM · Substrate—vegetation relations

Introduction

In arid and semiarid lands, water availability is the primary determinant of the spatial and temporal distributions of varying levels in productivity. Classical discussions of this relation have emphasized the ability of the vegetation to respond to sporadic pulses of precipitation (Noy-Meir 1973) and the limitation of such response to above-threshold events (Ogle and Reynolds 2004). At broad temporal and geographic scales, the vegetation in much of northwestern México is responsive to two climatic regimes, namely rains from tropical summer circulations, and winter rains from large cold fronts driven by the temperate westerlies. These responses are generally supported by low-resolution satellite imagery (NOAA-AVHRR Salinas-Zavala et al. 2002), and by highly processed MODIS satellite products like fPAR and net primary productivity (Turner et al. 2006). The quantitative analysis, however, has been limited by the paucity of weather stations. This problem might be mollified by the Tropical Rainfall Measurement Mission (TRMM, Huffman et al. 2007),

V. M. Rodríguez-Moreno División de Ciencias de la Tierra, Centro de Investigación Científica y de Educación Superior de Ensenada, BC (CICESE), Carretera Ensenada-Tijuana 3918, 22860 Ensenada, Baja California, México

V. M. Rodríguez-Moreno (☒)
Campo Experimental Pabellón, Instituto Nacional de
Investigaciones Forestales, Agrícolas y Pecuarias (INIFAP),
km 32.5 Carretera Aguascalientes-Zacatecas,
Pabellón de Arteaga, Aguascalientes, México
e-mail: rodriguez.victor@inifap.gob.mx

S. H. Bullock

Departamento de Biología de la Conservación, División de Biología Experimental y Aplicada, Centro de Investigación Científica y de Educación Superior de Ensenada, BC (CICESE), Carretera Ensenada-Tijuana 3918, 22860 Ensenada, Baja California, México

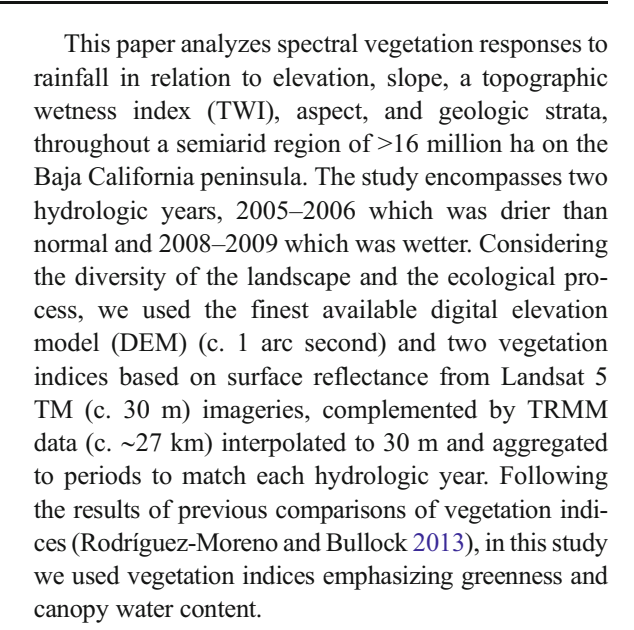


which provides continuous satellite-based data since 1997.

More recently, the importance of soil water has been emphasized in considering the effect of different sizes and frequencies of precipitation pulses (Knapp et al. 2008), because the storage of water affects the strength and duration of plant response. Although models of subsurface moisture flux are difficult to parameterize, particularly over varied topography in arid environments, general topographic attributes are readily derived (though scale dependent) from widely available digital elevation models (Franklin et al. 2000; van Asch et al. 2001). Two fundamental variables of substrate are useful indicators of moisture availability or moisture stress: slope gradient, which affects runoff, drainage, and soil development, erosion and deposition, and elevation, which affects precipitation and temperature. Thus, at a given elevation, slope should be inversely related to infiltration and soil depth, and for a given slope, moisture input should be greater at higher elevation and evaporation should decrease.

An additional complication in understanding the primary productivity of some arid regions is the diversity of plant adaptations to drought stress (Cowling et al. 1998; Díaz et al. 1998; Ghazanfar 1991; Schulze 1982) which result in a variety of short-term responses, seasonal phenologies, and interannual dependencies. Thus, the variability of vegetation response to precipitation and soil moisture variability might be expected to differ between desert grasslands, shrublands, and vegetation of mixed woody deciduous, evergreen, succulent, and herbaceous plants (Jobbágy et al. 1996). These may be reasons why most studies of productivity focus on sites with a low mixture of life forms, featureless topography, and substantial spatial continuity.

The central region of the Baja California peninsula is an exceptional region for the study of such issues. The peninsula extends 1,100 km from intra tropical to low temperate latitudes, and is affected, on north–south and east–west gradients, by tropical, temperate, regional, and local circulations (Dettinger 2004; Douglas et al. 1993; Farfán 2005; Salinas-Zavala et al. 2002). The east–west gradient is sustained by the warm waters of the Gulf of California, contrasting with the cool current and upwellings along the Pacific coast (Zaytsev et al. 2003). The center of the peninsula, comprising the Vizcaíno subregion of the Sonoran Desert (Shreve 1964), is notable for the variety of plant life forms in most areas (Peinado et al. 2005; Shreve 1964; Turner and Brown 1982).



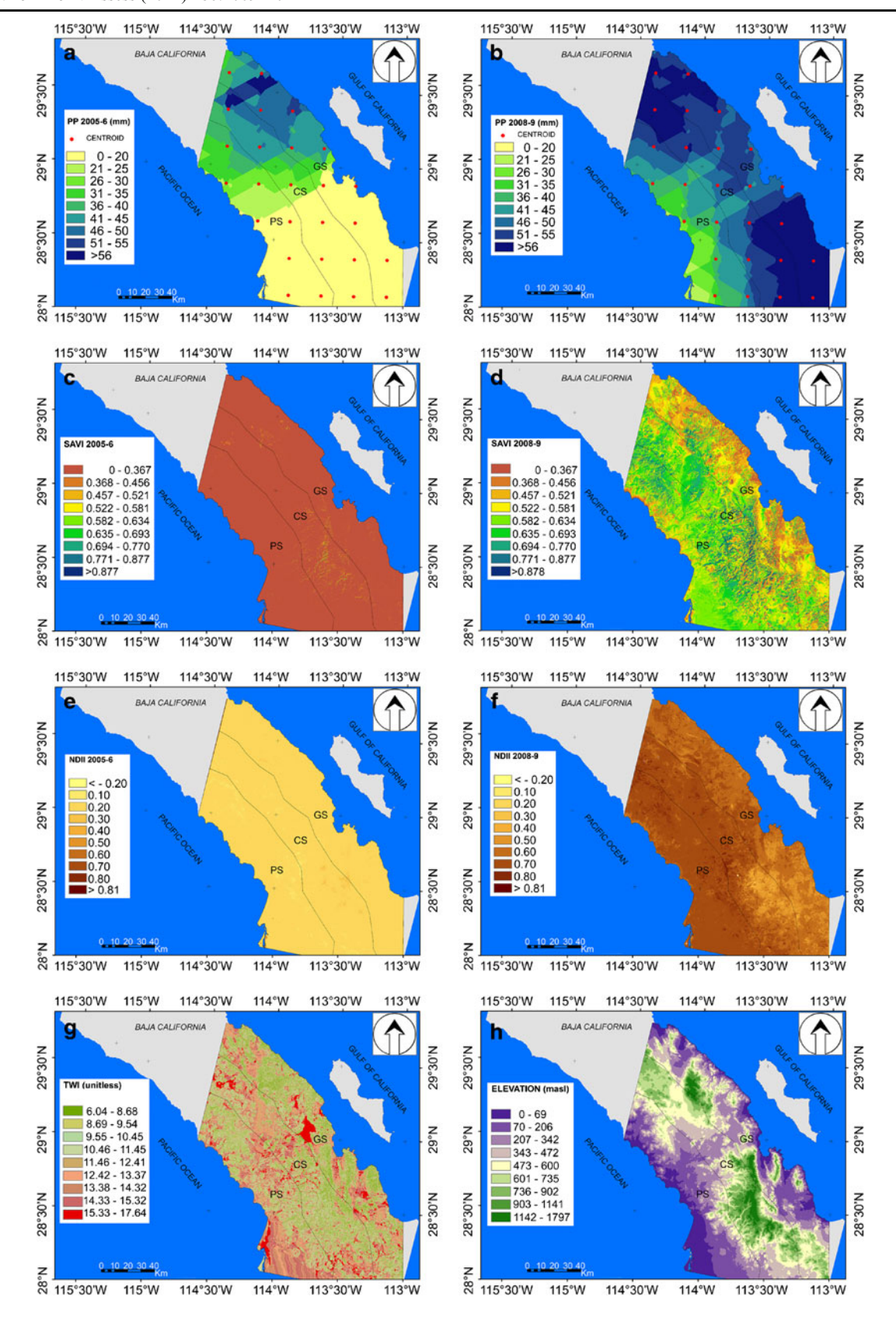
Materials and methods

The study area was in northwestern México on the Baja California peninsula. The limits were defined by the peninsular land in Landsat 5 TM images designated path 37 row 40 (Fig. 1). The area comprised 16,597 km² (592,748,259 Landsat 5 TM pixels) and included all or most of 26 pixels in TRMM imageries. The sites for present study were a random selection of 5,000 Landsat 5 TM pixels.

The area was subdivided into three major subregions: Pacific Ocean coast (PS), Gulf of California coast (GS), and Central (CS). The spatial limits of each subregion were conceived in relation to the coastlines as almost regular swaths of ~35 km. Soils were compared among these subregions, using the full-profile data collected for many sites by INEGI. Soil analyses showed that PS and CS share a more argillic texture than GS (sandy at 70 %). Organic matter was higher on the PS (0.65) than CS (0.53) or GS (0.50). Cation exchange capacity was higher for GS than the other two regions (respectively, 15.9, 13.6, 11.4), but there was not much variation in pH (c. 7.6).

Fig. 1 Regional maps of precipitation and vegetation indices. *Left* ▶ *column* 2005–2006; *right column* 2008–2009. **a, b** "Annual" sum of TRMM-estimated precipitation, interpolated by kriging. **c, d** "Annual" maximum SAVI. **e, f** "Annual" maximum NDII. **g** TWI. **h** Elevation. Spatial divisions are shown (PS, CS, and GS)







The geomorphic variables of elevation, slope, aspect, and TWI were based on a DEM with a resolution of one arc second (~30 m; data from Instituto Nacional de Estadística y Geografía (INEGI), Aguascalientes, México). Due to a strong relationship between slope and the resulting TWI, we decided not to include slope in later results. Because aspect is a circular variable, the aspect data were linearized for analysis, by creating two variables, "northness" and "eastness" as follows: northness = cos(aspect); eastness = sin(aspect). Northness takes values close to 1 if the aspect is close to north, close to –1 for southward and close to 0 for east or west. Eastness behaves similarly except that 1 represents due east facing slopes (Palmer 1993).

The DEM was corrected for sink and peak values (respectively, single pixels or neighborhoods of pixels with no exit for surface run-off, and small, isolated pixels or neighborhoods with relatively very high elevation) by comparing the altitudes in a DEM with the flow directions in a grid, to identify any inconsistencies. If flow direction indicated downward slope but altitudes indicated an upward slope, the DEM was lowered by a slight value (0.0001) until the contradiction vanished (Schaüble 2000). Topography provides an alternative for mapping spatial patterns of wetness in catchments where the assumption holds that groundwater tables basically follow topography (Haitjema and Mitchell-Bruker 2005). Several terrainbased wetness indices have been proposed to predict the spatial organization of soil moisture (Temimi et al. 2010). We used the TWI developed originally by Beven and Kirkby (1979) within the runoff model TOPMODEL. It is defined as $ln(a/tan\beta)$ where a is the local upslope area draining through a certain point per unit contour length and tanß is the local slope. The TWI has been used to study spatial scale effects on hydrological processes (Beven et al. 1988; Famiglietti and Wood 1991) and to identify hydrological flow paths for geochemical modeling (Robson et al. 1992) as well as to characterize biological processes such as annual net primary production (White and Running 1994) and vegetation patterns (Zinko et al. 2005). TWI is a unitless index and was designed to forecast possible saturated areas where runoff is dominated by subsurface flows; for greater values of TWI, the probability is higher of the pixel containing water from subsurface and surface runoff.

The temporal dynamics of vegetation both through and between hydrologic cycles were followed using 23

Landsat 5 TM imageries of two cycles (October 2005 through May 2006 and July 2008 to May 2009). Image dates for the 2005–2006 cycle comprised October 2, November 3, November 19, January 22, February 23, April 12, April 28, and May 14. Image dates for the 2008–2009 cycle were July 6, August 7, September 8, October 10, October 26, November 11, December 29, January 14, January 30, March 03, March 19, April 04, April 20, and May 06. All data collected were treated for radiometric, environmental, atmospheric, and topographic correction, applied in ERDAS v.9.2 (Rodríguez-Moreno and Bullock 2013). It is necessary to apply all these treatments to get surface reflectance data that closely represent the soil and cover physical and biochemical properties to light stimuli through remotely sensed data. A relative radiometric correction was used, applying satellite parameters, and not requiring simultaneous in situ data (Rodríguez-Moreno and Bullock 2013). The environmental correction compensated for image-unique acquisition conditions such as time of year, sun angle, and level of atmospheric-haze; it is also used in single scenes because the energy detected by the sensor is not the same as the energy actually reflected, due to scattering, absorption, and distortions (ERDAS 2008). The atmospheric correction was the simple and generalized technique of subtracting the darkest pixel value from all pixels in each band (Chavez 1988). The topographic or illumination correction accounted for the variation in reflectance due to angles between the sun, observed plane, and sensor. The solar irradiance incident on a slope varies strongly with slope azimuth relative to the sun and reflectance of the slope varies with the incidence angle, between the solar vector and the slope normal (Vincini et al. 2011). The topographic or illumination correction was necessarily computed for each date because of the changes in sensor and sun angles relative to the ground (Rodríquez-Moreno and Bullock 2013).

For this study we used two vegetation indices. The Soil Adjusted Vegetation Index (SAVI; Eq. 1) is closely related to the greenness-responsive Normalized Difference Vegetation Index (Rodríguez-Moreno and Bullock 2013) but attempts to lessen the effect of soil brightness by means of a parameter (*L*) which depends on the extent of vegetation cover (Bannari et al. 1995). This adjustment is of particular importance for semiarid ecosystems where cover is incomplete to extremely scant. The other index was the Normalized Difference Infrared Index (Eq. 2) which has shown significant correlation



with leaf water content (Hardinsky et al. 1983; Serrano et al. 2000) and is apparently sensitive to variation in the character of landscape cover in arid regions (Rodríguez-Moreno and Bullock 2013).

$$SAVI = \frac{(NIR - RED) * 1.7}{(NIR + RED + 0.5)} \tag{1}$$

$$NDII = \frac{NIR - SWIR}{(NIR + SWIR)} \tag{2}$$

In Eqs. 1 and 2, NIR stands for near infrared (0.76–0.90 μ m), R stands for red (0.63–0.69 μ m), L represents soil cover (here set at 0.7), and SWIR stands for shortwave infrared (1.55–1.75 μ m). SAVI ranges from 0 to 1 and NDII from –1 to +1; lower values of NDII mean less canopy water. Data were processed for all pixels in the region for all available dates in the two cycles. The maximum value of each index for each pixel in each of the 2 years was obtained for analysis the relation of the indices to rainfall and terrain. To minimize the co-register bias of the DEM and rainfall estimate (see below) with the Landsat imageries, accumulated rainfall and terrain factors were interpolated and re-sampled, respectively, in accordance with their respective spatial resolutions.

Precipitation data were derived from satellite observations of the Tropical Rainfall Measurement Mission (Huffman et al. 2007, Kummerow et al. 1998, Wolff et al. 2005). TRMM data products include 3-hourly, daily, monthly, and annual totals for points on a 0.25° by 0.25° grid extending from 50° S to 50° N latitude (Kempler 2011). Estimated precipitation was summed over the period of September 30, 2005 to April 30, 2006, to represent the year 2005–2006 and from August 1, 2008 to April 30, 2009 to represent the year 2008–2009. These values were assigned to the calculated centroids of TRMM's grid cells (spacing of c. 27.5 km). Then accumulated rainfall was interpolated between centroids by the Ordinary Kriging technique. Kriging has been widely used by geostatisticians for spatial estimation of rainfall (Sun et al. 2003). Statistical regional analysis for each strata mask was performed on a basis of 5,000 randomly located points distributed throughout the study area.

Regarding the statistical analysis of the data, we applied Spearman R rank correlation tests, Kruskal–Wallis ANOVA rank tests, Dunn's test, and multiple regression analysis. For regression models, a forward stepwise procedure was applied.

Results

Regional overview of rainfall, vegetation indices and terrain factors

Although in both years the TRMM-estimated rainfall was well below 100 mm, there was a difference of more than twofold in the regional means, while the variation among sites was much greater in the drier year (Table 1). Mean SAVI was almost three times higher in the wetter year, as was its variation, while NDII increased greatly from a negative mean without a change in variation.

Regional topography was centered on modest elevations with only 10 % of the surface exceeding 800 m (Table 1). Low slope gradients were typical, with more than 16 % of the surface being flat and more than 90 % had a slope below 25 %. Exposures tended to be bimodal, in both N-S and E-W directions. The principal substrates were extrusive igneous rocks (25 %), alluvium (22 %), conglomerates and sandstones (21 %), intrusive igneous rocks (20 %), and metamorphic rocks (9 %) with minor amounts of soils underlain by petrocalcic layers (2 %) and limestone (1 %). There was not much variation in soil pH in the region (7.7±0.6) and log sodium saturation (%) was low (0.48±0.45). Soil texture showed a fairly broad variation (% clay=15.5±11.7, range 2-52 %) and the soils sampled were generally shallow (21±15 cm). There were some important differences of soils between subregions: PS and CS shared a higher clay content than GS which showed an average of 70 % sand. Organic matter was higher on the PS (0.65) than CS (0.53) or GS (0.50). Cation exchange capacity (CEC) was higher for PS than the other two regions (respectively, 15.9, 13.6, and 11.4).

For precipitation, the grid of data points and krigged interpolation are presented in Fig. 1 along with the vegetation indices, showing a pronounced regionalization, particularly for precipitation. Some of this variation reflects the division of Gulf, Cordillera, and Pacific subregions. The maps confirm the strong contrast between the 2 years for rain, greenness, and vegetation wetness and strongly suggest that the maximum values of vegetation indices were not closely related to estimated total precipitation. Comparison of the TWI (Fig. 1g, h) demonstrated an association of high elevation with lower TWI and vice versa. With the exception of a few large plains and endorrheic basins, moderate and higher values of TWI were well-dispersed across this complex landscape.



Table 1 Regional descriptive statistics in both cycles and terrain factors

	Regional mean	10th percentile	90th percentile	Standard deviation	Skewness
Pacific subregion					
PP 2005-6	17.5	5.4	34.4	11.6	0.42
SAVI 2005-6	0.18	0.15	0.22	0.04	2.59
NDII 2005-6	-0.12	-0.18	-0.06	0.06	1.89
PP 2008-9	39.7	27.4	49.5	8.0	-0.28
SAVI 2008-9	0.61	0.51	0.71	0.09	0.52
NDII 2008-9	0.55	0.51	0.59	0.04	0.94
TWI	12.2	9.2	14.9	2.1	-0.24
Elevation	236	35	498	175	0.80
Slope	6.5	0.0	17.8	7.9	1.5
Northness	0.14	-0.95	1.00	0.76	-0.19
Eastness	-0.15	-0.95	0.80	0.60	0.28
Central subregion					
PP 2005-6	20.95	2.74	44.88	17.72	0.37
SAVI 2005-6	0.21	0.16	0.28	0.06	2.85
NDII 2005-6	-0.09	-0.17	0.01	0.09	4.18
PP 2008-9	53.63	44.74	62.97	6.39	0.10
SAVI 2008-9	0.61	0.47	0.73	0.12	0.96
NDII 2008-9	0.50	0.39	0.59	0.08	-1.24
TWI	11.65	8.84	14.80	2.19	0.18
Elevation	614	318	940	251	0.77
Slope	9.6	0.0	25.3	10.2	1.19
Northness	0.02	-0.96	1.00	0.76	0.03
Eastness	-0.08	-0.95	0.88	0.64	0.15
Gulf subregion					
PP 2005-6	26.13	3.22	49.31	19.13	0.06
SAVI 2005-6	0.19	0.15	0.25	0.05	1.73
NDII 2005-6	-0.04	-0.10	0.04	0.07	4.15
PP 2008-9	56.67	49.30	66.52	6.14	0.37
SAVI 2008-9	0.53	0.39	0.67	0.12	0.49
NDII 2008-9	0.46	0.38	0.53	0.06	-0.24
TWI	11.36	8.56	14.85	2.34	0.32
Elevation	413	100	774	274	1.05
Slope	11.4	0.0	27.5	10.7	0.79
Northness	0.19	-0.90	1.00	0.71	-0.32
Eastness	0.05	-0.93	0.96	0.67	-0.09

Longitudinal contrasts in precipitation and vegetation

Spatial interpretations of greenness and vegetation wetness in both cycles showed an interesting dynamic in the plant communities, with longitudinal contrasts across the peninsula, especially in the wetter year. Total precipitation, NDII, and SAVI were all heterogeneous

between years and among subregions in both years (Kruskal–Wallis tests, all p<0.001). The highest precipitation was clearly in GS in both years (Fig. 2).

The highest mean SAVI occurred in the CS in both years, and the differences in SAVI among subregions did not parallel the differences in precipitation (Fig. 2). NDII exhibited only negative values for the drier year



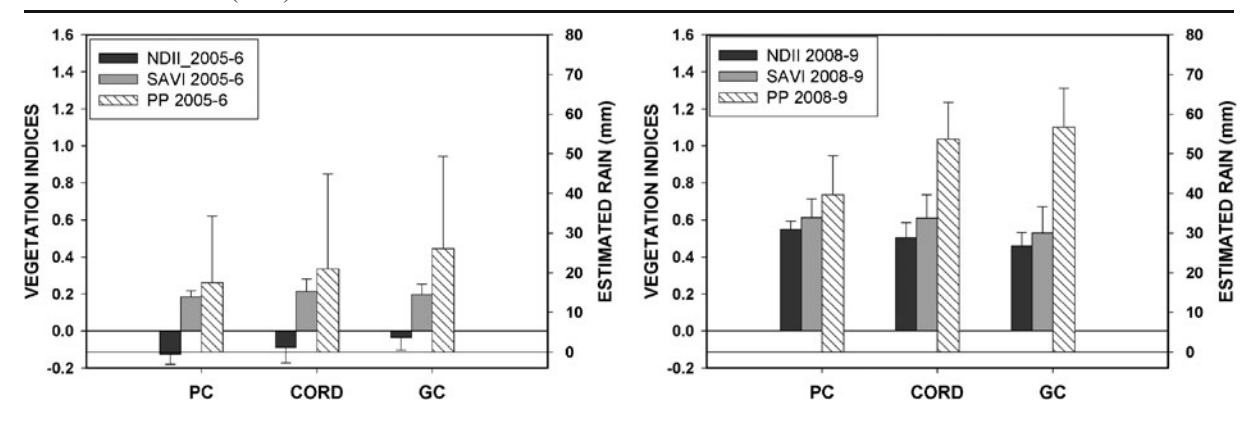


Fig. 2 Regional variation in estimated "annual" precipitation and VI's, with 2005–2006 at *left* and 2008–2009 at *right* (whisker ± 0.95 confidence interval)

in all three subregions, although the trend was parallel to precipitation. For the wetter year, the pattern of NDII was opposite to precipitation, with the highest mean in the PS, reaching almost 0.44 in striking contrast to the drier year, while CS and GS showed successively lower values.

As shown by Fig. 2 and suggested by Fig. 1, there was a striking difference in the amount of estimated rain between years and among subregions. In the drier year, SAVI was not so different among regions, despite the fact that estimated rain for the GS was substantially greater than for either the PS or CS. In contrast, mean NDII directly followed the trend in precipitation. For the wetter year, the GS also received more precipitation than the PS and CS but the mean of maximum values of SAVI were lower in the GS. Moreover, maximum NDII showed a trend opposite to precipitation in this year. Clearly, total precipitation alone, as estimated by TRMM, was not a consistently dominant factor for the physiological condition of the vegetation in this region.

Statistical analysis

Based on the Kolmogorov–Smirnov test, none of the variables was strictly normal (Table 1), although the vegetation indices were close to normal. Precipitation showed a weak tendency to bimodality in 2008–2009 with a possible minor mode at low values, and a very strong bimodality in 2005–2006. Elevation was skewed to low values, with its mode in the range of 400 m. Slope was strongly skewed with its mode in the lowest class. TWI presented the most uniform distribution, mostly limited to values between 8 and 15. Northness and eastness were mostly uniform but did show some

excess of north and south and of east and west exposures. Both non-parametric and parametric analyses were performed. In some cases log transformations of elevation and slope (slope+1) were used.

Rank correlations among the variables are presented in Table 2. TWI had a strong negative correlation with slope, as expected by definition; it also had modest correlations with elevation and northness. Elevation had a moderate positive correlation with slope and with total estimated precipitation in 2008-2009 but not 2005-2006; unexpectedly, its strongest correlation with a vegetation index was for SAVI in the drier year, and it was better related to SAVI than to NDII in both years. Slope was more closely related to NDII but with opposite signs in the 2 years, and also tended to be lower for more northerly exposed hillsides. Exposure did not stand out in the matrix, but correlations of eastness with precipitation and vegetation indices were all greater than for northness. Precipitation appeared to be among the best correlates of the vegetation indices, particularly for 2008-2009 and for NDII. Reassuringly, the vegetation indices were moderately well-correlated between years and with each other.

The relationships of the maximum values of the vegetation indices to total precipitation were also examined using the continuous variables in simple linear regression (Table 3). The analyses for 2005–2006 were not performed because of the strongly bimodal distribution of precipitation. Regionally for 2008–2009, SAVI showed a highly significant but extremely weak and unexpectedly negative relation to precipitation. For NDII, the relation was also negative but much stronger and noticeably skewed from linear at precipitation sums less than 40–45 mm. Among subregions,



Table 2 Spearman rank correlation matrix

	TWI	Elev.	Slope	North.	East.	PP 05-6	PP 08-9	SAVI 05-6	SAVI 08-9	NDII 05-6
Elevation	38									
Slope	91	.43								
Northness	.24	23	24							
Eastness	.02	02	.01	.04						
PP 05-6	07	.01	.06	0	.05					
PP 08-9	13	.42	.17	04	.11	06				
SAVI 05-6	02	.39	.11	.01	03	11	.21			
SAVI 08-9	.08	.12	06	01	13	04	21	.50		
NDII 05-6	19	.13	.24	.01	.06	.03	.42	.10	53	
NDII 08-9	.09	08	14	04	06	.20	52	09	.55	83

however, the relations were heterogeneous. SAVI showed very weak positive and negative relations in PS and CS, respectively, but no significant relationship in GS. In contrast, NDII showed a non-significant relation in PS and stronger, negative relations in CS and GS.

With log transformation of the elevation and slope gradient variables, least-squares multiple linear regression was used to simultaneously evaluate the effects of all the terrain variables and precipitation (Table 4). Following the previous indications of systematic differences between the subregions, the analysis was done by subregion. It also should be noted that despite the regional correlations in Table 2, colinearity was not equal among subregions. For example, precipitation and elevation were moderately correlated in the PS but this was much reduced in CS and virtually absent

Table 3 Regression of pixel maximum vegetation index on total annual precipitation 2008–2009

	Regression <i>F</i> , <i>p</i>	r^2	Coefficient	Standard error of estimate
SAVI				
Regional	103, < 0.001	0.02	-0.002	0.117
PS	87, < 0.001	0.05	0.003	0.089
CS	26, < 0.001	0.02	-0.002	0.122
GS	1, =0.340			
NDII				
Regional	1,408, < 0.001	0.22	-0.003	0.065
PS	67, < 0.001	0.04	0.001	0.039
CS	220, < 0.001	0.12	-0.005	0.078
GS	329, < 0.001	0.15	-0.004	0.057

in GS (respectively, r=0.64, 0.17, and 0.01). The relation of slope to elevation was somewhat less toward the east (r=0.48, 0.46, and 0.34). The regression analyses were made with the full models, not stepwise, and did not include interaction terms.

None of these models explained more than 20 % of the variation in vegetation indices; the strongest were for NDII in the CS and GS. Also, none of the factors was significant in all the models. Surprisingly, the weakest factors in general were exposition, with both northness and eastness failing to affect the NDII model and northness failing for SAVI in two of the subregions. It was also surprising that none of the factors operated in the same sense (that is, always positive or always negative coefficient) for all subregions and both indices. Thus the generally but not universally significant factors of precipitation, elevation, Topographic Wetness Index, and slope were apparently related to the indices in both positive and negative directions in different cases. Their coefficients were generally in the range of 0.002 to 0.033, compared to 0.159 to 0.993 for the models' constants.

Models based on the two main rock types and subregion produced generally better results (Table 5). For SAVI, all subregions and both rock types showed significant results that were occasionally better than the general models of Table 4. The best results were for the Pacific subregion, where elevation and slope added power. For SAVI on the extrusive igneous sites, precipitation was not a significant factor, but slope (and TWI) figured in all the models, which was unexpected because these sites are often mesa tops and must have more clay in the soil than granitic sites. For NDII,



Table 4 Multiple regression analysis for 2008–2009

	SAVI			NDII			
	Pacific	Cordillera	Gulf	Pacific	Cordillera	Gulf	
Regression F	29.4	10.8	26.7	25.6	62.4	75.1	
Multiple adjusted r^2	0.10	0.04	0.08	0.09	0.19	0.20	
Constant t	9.67	6.95	3.11	33.2	23.0	25.2	
Precipitation total		-4.9			-13.9	-20.1	
TWI	2.55	3.92	5.06	-3.8	-2.5		
Log elevation	8.38	1.07*	9.68	6.8	-5.0	8.3	
Log slope+1		4.2	3.2	-2.9	-5.2	-4.1	
Northness			4.1				
Eastness	-2.7	-4.0	-4.1				
N pixels	1,578	1,603	1,819	1,578	1,603	1,819	

The values shown for the constants and each factor are t, and only values with p < 0.05 are shown. Negative values of t are associated with negative coefficients

Table 5 Multiple regression analysis for SAVI and NDII in 2008–2009 on sites with intrusive or extrusive igneous rocks

	Intrusive igneous			Extrusive igneous			
	Pacific	Cordillera	Gulf	Pacific	Cordillera	Gulf	
SAVI							
Regression F	5.1	2.8	9.2	12.7	4.0	5.8	
Multiple adjusted r^2	0.10	0.03	0.12	0.16	0.04	0.06	
Constant t	1.8	3.2					
Precipitation total		-2.8	-2.0				
TWI			2.2	2.2	2.8	2.2	
Log elevation	3.2		5.7	5.3		3.8	
Log slope+1				2.9	4.0	2.2	
Northness			2.3			2.6	
Eastness		-2.3	-2.7			-2.3	
NDII							
Regression F	13.6	25.0	34.1	13.6	15.2	12.5	
Multiple adjusted r^2	0.24	0.26	0.35	0.17	0.17	0.13	
Constant t	9.9	11.1	12.2	8.8	10.4	11.6	
Precipitation total		-7.8	-12.6	2.9	-5.7	-8.1	
TWI		-2.9					
Log elevation	7.0		5.5	6.1	-5.3		
Log slope+1		-5.3	-2.6				
Northness							
Eastness		-2.1					
N pixels	234	405	372	360	407	471	

The values shown for the constants and each factor are t, and only values with p < 0.05 are shown. Negative values of t are associated with negative coefficients



precipitation was important on both rock types, followed by elevation, and the models were all among the strongest found, accounting for 24–35 % of the variation in NDII on intrusive igneous rocks.

An independent approach to the analysis of imageries for the region relied not on the 5,000 points but on categorization of the entire gridded landscape by elevation, slope and subregion, and non-parametric comparison (Kruskal–Wallis and Dunn tests) among these categories with regard to precipitation and vegetation indices in the same landscape units. Despite the complexity of pairwise tests and the categorization including both elevation and slope, the results tended to support the conclusions that precipitation effects were not universal or consistently positive, that elevation was often a positive factor but slope was more complex, and that the three subregions were not strictly parallel in factors affecting vegetation development.

Discussion

The remotely sensed imageries of vegetation characteristics and rain, together with the best-available fine-scale DEM allowed the measurement of the dependence of the former on climate and terrain features, in periods of contrasting moisture availability. Our findings do not reflect simple relations of accumulated precipitation and runoff to vegetation development. Marked differences were observed within and among the subregions, and between years. For both years, although the GS subregion received more rain than the other two, it showed lower maximum greenness and canopy water content. Moreover, the PS had higher maximums of both indices in the wetter year, despite much lower rainfall. For the drier year on the PS, despite receiving less than 20 mm of rain, greenness was almost equal to the other two subregions. In regard to these apparent inconsistencies, both climate and soil may be important contributing factors.

The geological substrate is clearly relevant, probably affecting both water and nutrient availability in relation to variations in derived soil texture and nutrient content (Bisigato et al. 2009; Monger and Bestelmeyer 2006; Osterkamp 2008) as well as surface and subsurface fissuring (Witty et al. 2003). As noted above, soils are generally much sandier on the GS, facilitating faster and deeper drainage of water and consequently low soil water retention. Greater clay content on the PS and

CS should favor slower drainage, greater retention, and perhaps better use of smaller rainfall events. Nutrient availability should also be affected by texture, as exemplified here by CEC. How nutrient cycling is affected by episodic water availability is not generally well known (Austin et al. 2004; Borken and Matzner 2009) and clearly merits study in the present region. At a larger scale, the Topographic Wetness Index was directly related to SAVI in all three subregions, but inversely related to NDII in two and not significantly related on the GS. In this regard, we should emphasize that the coefficients for TWI, as for the other terrain factors and for precipitation to a lesser extent, were extremely low. Clearly, methods need to be tested here to approximate soil depth, texture, and moisture (De Jeu et al. 2008).

The spatial pattern in vegetation dynamics may be influenced not only by rain, geomorphic, and soil factors, but also by factors that affect surface and air temperature, like moist and cool winds from the Pacific Ocean, their adiabatically dried remnants on the Gulf slope, and warmer air along the Gulf of California. These persistent differences in temperature and humidity may play an important role in reducing fluctuations in the vegetation near the Pacific coast. The Cordillera subregion is undoubtedly more complex than either coast, at least because elevation and topography must add complexity to the effect of ventilation by the Pacific marine layer, and may also increase precipitation from northern and southern storms. Of course, subregional and local climatic patterning are likely to be reflected in other properties and processes of the ecosystem which affect vegetation indices and require more specific and local study, such as microbial activity, nutrient cycling, root dynamics, and radiative transfer of various life forms (Huxman et al. 2004).

The results for the sampled years do require interpretation, but longer-term patterns may contribute important elements. For at least the 50–60 years of instrumental record, the Pacific slope had a higher average annual rainfall than the Gulf slope, and even El Niño years had more enhancement of precipitation in winter (northwest to southeast) than summer (southeast to northwest) (Minnich et al. 2000). Together with the temperature gradient, this suggests that cover (both canopy extent and leaf area index) should be higher on the Pacific slope, and thus the potential response to pulses of water availability might be greater.

The tendency among subregions for negative relationships of both vegetation indices with precipitation



in the wetter year might be explained from several points of view. The negative relations were of very low power, based on annual data, and geographically broad-scale; thus, it cannot be inferred that any particular site would show such a pattern over the course of one or many years. However, despite the generally negative (or curved) in relation to precipitation, vegetation wetness followed a pattern very loosely parallel to greenness. Of course, water from precipitation becomes available through the soil, so that the temporal patterns of precipitation, infiltration, evaporation, drainage, and run-off are important considerations. Intense rainfall, above some amount dependent on slope and soil, may have been partly unusable. Moreover, the data here are maximums of the vegetation indices, and their values in the relatively wet year were substantially above values from the same sites in 2005–2006. In any event, there is evidence that NDII can closely estimate canopy Equivalent Water Thickness, such that changes in its values can be detected during drought (Ceccato et al. 2002; Hunt and Yilmaz 2007). The present study suggests that the relation of metabolism to NDII, in contrasting plant communities, merits further study. Variations in vegetation composition regarding physiology and form probably underlie the strong negative correlation of NDII between the 2 years (r=-0.79), with the highest (but moderate) values in 2005-2006 associated with similar values in 2008-2009, while sites with higher NDII in the wetter year had lower values in the drier year. SAVI, in contrast showed a positive (but weaker) correlation between years (r=0.60).

Water availability in arid regions is both sporadic and highly variable in intensity, and most rainy events are of very low magnitude and are doubtfully beneficial for vascular plants (Huxman et al. 2004; Tongway et al. 2004), although probably of importance to microflora (Karnieli et al. 1996; Rodríguez-Moreno and Bullock 2013). One of the consequences of the erratic nature of water inputs in arid ecosystems is that surface soils experience prolonged periods of drying followed by rapid rewetting (Austin et al. 2004). Plant communities must have evolved mechanisms not just to withstand drought but to capture and perhaps store water in the infrequent torrential events. Seasonal patterns of greenness and water content are undoubtedly complex, particularly among species and sites (Chesson et al. 2004; Franco-Vizcaíno 1994), and probably restrict the power of the relatively simple and geographic extensive models explored here.

Conclusions

This study applied analysis of fine-scale, remotely sensed surface reflectance grids to the characterization of spatial variation in the greenness and canopy water content of semi-desert vegetation at a regional scale. We tested its patterning according to major variables of the physical environment, including rainfall estimates from previously modeled radar data. The majority of variation remains unexplained, but the results strongly suggest that models will be of distinct form for different areas, almost certainly at scales finer than our subregions, and for different years and/or seasons. Additional climatic and substrate variables as wind, relative humidity, insolation (direct and diffuse), and tectonic (e.g., fissures) and geologic factors that influence soil properties and hydrologic processes, may also be crucial in reaching a more thorough understanding of the structure and abundance of the perennial and ephemeral vegetation and photosynthetic microbes. Regional environment indicators clearly need to be down-scaled to follow the patchy vegetation dynamics in regions of similar complexity, and diversified through new sensors.

Acknowledgments The authors express their gratitude to the Instituto Nacional de Investigaciones Forestales, Agrícolas y Pecuarias (INIFAP), the Centro de Investigación Científica y de Educación Superior de Ensenada (CICESE), the Secretaría de Medio Ambiente y Recursos Naturales, and the Consejo Nacional de Ciencia y Tecnología (SEMARNAT-CONACYT grant 23777) for their technical and financial support.

Open Access This article is distributed under the terms of the Creative Commons Attribution License which permits any use, distribution, and reproduction in any medium, provided the original author(s) and the source are credited.

References

Austin, A. T., Yahdjian, L., Stark, J. M., Belnap, J., Porporato, A., Norton, U., Ravetta, D. A., & Schaeffer, S. M. (2004). Water pulses and biogeochemical cycles in arid and semiarid ecosystems. *Oecologia*, 141, 221–235.

Bannari, A., Morin, D., Bonn, F., & Huete, A. R. (1995). A review of vegetation indices. *Remote Sensing Reviews*, 13, 95–120.

Beven, K. J., & Kirkby, M. J. (1979). A physically based, variable contributing area model of basin hydrology. *Hydrological Sciences Bulletin*, 24, 43–69.

Beven, K. J., Wood, E. F., & Sivapalan, M. (1988). On hydrological heterogeneity—catchment morphology and catchment response. *Journal of Hydrology*, 100, 353–375.



- Bisigato, A. J., Villagra, P. E., Ares, J. O., & Rossi, B. E. (2009). Vegetation heterogeneity in Monte Desert ecosystems: a multi-scale approach linking patterns and processes. *Journal* of Arid Environments, 73, 182–191.
- Borken, W., & Matzner, E. (2009). Reappraisal of drying and wetting effects on C and N mineralization and fluxes in soils. *Global Change Biology*, 15, 808–824.
- Ceccato, P., Flasse, S., & Gregoire, J. M. (2002). Designing a spectral index to estimate vegetation water content from remote sensing data: Part 2. Validations and applications. *Remote Sensing of Environment*, 82, 198–207.
- Chavez, P. S., Jr. (1988). An improved dark-object subtraction technique for atmospheric scattering correction of multispectral data. *Remote Sensing of Environment*, 24, 459–479.
- Chesson, P., Gebauer, R. L., Schwinning, S., Huntly, N., Wiegand, K., Ernest, M. S., Sher, A., Novoplansky, A., & Weltzin, J. F. (2004). Resource pulses, species interactions, and diversity maintenance in arid and semi-arid environments. *Oecologia*, 14, 236–253.
- Cowling, R. M., Rundel, P. W., Desmet, P. G., & Esler, K. J. (1998). Extraordinary high regional-scale plant diversity in Southern African arid lands: subcontinental and global comparisons. *Diversity and Distributions*, 4, 27–36.
- De Jeu, R. A. M., Wagner, W., Holmes, T. R. H., Dolman, A. J., Van De Giesen, N. C., & Friesen, J. (2008). Global soil moisture patterns observed by space borne microwave radiometers and scatterometers. Surveys in Geophysics, 29, 399–420.
- Dettinger, M. (2004). Fifty-two years of "pineapple express" storms across the west coast of North America (p. 20). La Jolla: U.S. Geological Survey.
- Diaz, S., Cabido, M., & Casanoves, F. (1998). Plant functional traits and environmental filters at a regional scale. *Journal* of Vegetation Science, 9, 113–122.
- Douglas, M. W., Maddox, R. A., Howard, K., & Reyes, S. (1993). The Mexican monsoon. *Journal of Climate*, *6*, 1665–1677.
- ERDAS. (2008). ERDAS Subpixel Classifier. White paper. http://geospatial.intergraph.com/Libraries/White_Papers/ IMAGINE_Subpixel_Classifier%E2%84%A2.sflb.ashx [Accessed: 07-06-2012]
- Famiglietti, J. S., & Wood, E. F. (1991). Evapotranspiration and runoff from large land areas—land surface hydrology for atmospheric general-circulation models. *Surveys in Geophysics*, 12, 179–204.
- Farfán, L. M. (2005). Development of convective systems over Baja California during tropical cyclone Linda (2003). Weather and Forecasting, 20, 801–811.
- Franco-Vizcaíno, E. (1994). Water regime in soils and plants along an aridity gradient in central Baja California, Mexico. *Journal* of Arid Environments, 27, 309–323.
- Franklin, J., McCullogh, P., & Gray, C. (2000). Terrain variables used for predictive mapping of vegetation communities in Southern California. In J.P. Wilson & J.C. Gallant (Eds), Terrain analysis. Principles and applications (pp. 331–353). New York: John Wiley & Sons.
- Ghazanfar, S. A. (1991). Vegetation structure and phytogeography of Jabal Shams, an arid mountain in Oman. *Journal of Biogeography*, 18, 299–309.
- Haitjema, H. M., & Mitchell-Bruker, S. (2005). Are water tables a subdued replica of the topography? Ground Water, 43, 781–786.
- Hardinsky, M. A., Klemas, V., & Smart, R. M. (1983). The influence of soil salinity, growth form, and leaf moisture on the spectral

- radiance of Spartina alterniflora canopies. Photogrammetric Engineering and Remote Sensing, 49, 77–83.
- Huffman, G. J., Adler, R. F., Bolvin, D. T., Gu, G., Nelkin, E. J., Bowman, K. P., Hong, Y., Stocker, E. F., & Wolff, D. B. (2007). The TRMM multisatellite precipitation analysis (TMPA): quasi-global, multiyear, combined-sensor precipitation estimates at fine scales. *Journal of Hydrometeorology*, 8, 38–55.
- Hunt, E.R., Jr., & Yilmaz, M.T. (2007). Remote sensing of vegetation water content using shortwave infrared reflectances. In: W. Gao & S.L. Ustin (Eds.), Remote Sensing and Modeling of Ecosystems for Sustainability IV. Proceedings of SPIE 6679, 667902.
- Huxman, T. E., Sneyder, K. A., Tissue, D., Leffler, A. J., Ogle, K., Pockman, W. T., Sanquist, D. R., Potts, D. L., & Schwinning, S. (2004). Precipitation pulse and carbon fluxes in semiarid and arid ecosystems. *Oecologia*, 141, 254–268.
- Jobbágy, E. G., Paruelo, J. M., & León, R. J. (1996). Vegetation heterogeneity and diversity in flat and mountain landscapes of Patagonia (Argentina). *Journal of Vegetation Science*, 7, 599–608.
- Karnieli, A., Shachak, M., Tsoar, H., Zaady, E., Kaufman, Y., Danin, A., & Porter, W. (1996). The effect of microphytes on the spectral reflectance of vegetation in semiarid regions. *Remote Sensing of Environment*, 57, 88–96.
- Kempler, S. (2011). Mirador data access made simple. http:// mirador.gsfc.nasa.gov/collections/TRMM_3B42__006.shtml Accessed: 3 November 2011.
- Knapp, A. K., Beier, C., Briske, D. D., Classen, A. T., Luo, Y., Reichstein, M., Smith, M. D., Smith, S. D., Bell, J. E., Fay, P. A., Heisler, J. L., Leavitt, S. W., Sherry, R., Smith, B., & Weng, E. (2008). Consequences of more extreme precipitation regimes for terrestrial ecosystems. *BioScience*, 58, 811–821.
- Kummerow, C., Barnes, W., Kozu, T., Shiue, J., & Simpson, J. (1998). The tropical rainfall measuring mission (TRMM) sensor package. *Journal of Atmospheric and Oceanic Technology*, 15, 809–817.
- Minnich, R. A., Franco-Vizcaíno, E., & Dezzani, R. J. (2000). The El Niño/Southern Oscillation and precipitation variability in Baja California, México. *Atmosfera*, 13, 1–20.
- Monger, H. C., & Bestelmeyer, B. T. (2006). The soilgeomorphic template and biotic change in arid and semiarid ecosystems. *Journal of Arid Environments*, 65, 207– 218.
- Noy-Meir, I. (1973). Desert ecosystems: environment and producers. Annual Review of Ecology and Systematics, 4, 25–51.
- Ogle, K., & Reynolds, J. F. (2004). Plant responses to precipitation in desert ecosystems: integrating functional types, pulses, thresholds, and delays. *Oecologia*, 141, 282–294.
- Osterkamp, W. R. (2008). Geology, soils, and geomorphology of the Walnut Gulch Experimental Watershed, Tombstone, Arizona. *Journal of the Arizona-Nevada Academy of Science*, 40, 136–154.
- Palmer, M. W. (1993). Putting things in even better order: the advantages of canonical correspondence analysis. *Ecology*, 74, 2215–2230.
- Peinado, M., Delgadillo, J., & Aguirre, J. L. (2005). Plant associations of the El Vizcaíno Biosphere Reserve, Baja California Sur, México. Southwestern Naturalist, 50, 129–149



- Robson, A., Beven, K., & Neal, C. (1992). Towards identifying sources of subsurface flow: a comparison of components identified by a physically based runoff model and those determined by chemical mixing techniques. *Hydrological Processes*, 6, 199–214.
- Rodríguez-Moreno, V. M., & Bullock, S. H. (2013). Comparación espacial y temporal de índices de la vegetación para verdor y humedad y aplicación para estimar LAI en el Desierto Sonorense. Revista Mexicana de Ciencias Agrícolas, 4, 611– 623
- Salinas-Zavala, C. A., Douglas, A. V., & Diaz, H. F. (2002). Inter-annual variability of NDVI in Northwest Mexico: associated climatic mechanisms and ecological implications. Remote Sensing of Environment, 82, 417–430.
- Serrano, L., Ustin, S. L., Roberts, D. A., Gamon, J. A., & Peñuelas, J. (2000). Deriving water content of chaparral vegetation from AVIRIS data. *Remote Sensing of Environment*, 74, 570–581.
- Schaüble, H. (2000). Erosionsmodellierungen mit GIS. Probleme und Lösungen zur exakten Prognose von Erosion und Akkumulation. In H.J. Rosner (Ed.), GIS in der Geographie II. Ergebnisse der Jahrestagung des Arbeitskreises GIS (25– 26), 51–62. Tübingen: Geographisches Institut der Universität.
- Schulze, E. D. (1982). Plant life forms and their carbon, water and nutrient relations. In O. L. Lange, P. S. Nobel, C. B. Osmond, & H. Ziegler (Eds.), *Physiological Plant Ecology II. Water Relations and Carbon Assimilation* (pp. 616– 676). Berlin: Springer.
- Shreve, F. (1964). Vegetation of the Sonoran Desert. In F. Shreve & I. L. Wiggins (Eds.), *Vegetation and Flora of the Sonoran Desert* (pp. 6–186). Stanford: Stanford University Press.
- Sun, X., Manton, M.J., & Ebert, E.E. (2003). Regional rainfall estimation using double-krigging of raingauge and satellite observations. Bureau of Meteorology Research Centre. Report 94. 36 p.
- Temimi, M., Cortina, J., Chaouch, N., Sukumal, P., Khanbilvardi, R., & Brissette, F. (2010). A combination of remote sensing data and topographic attributes for the spatial and temporal monitoring of soil wetness. *Journal of Hydrology*, 388, 28– 40.

- Tongway, D. J., Cortina, J., & Maestre, F. T. (2004). Heterogeneidad especial y gestión de medios semiáridos. *Ecosistemas*, 13, 2– 15
- Turner, D. P., Ritts, W. D., Maosheng, Z., Kurc, S. A., Dunn, A. L., Wofsy, S. C., Small, E. E., & Running, S. W. (2006). Assessing interannual variation in MODIS-based estimates of gross primary production. *Geoscience and Remote Sensing*, 44, 1899–1907.
- Turner, R.M., & Brown, D.E. (1982). Sonoran desertscrub. In D.E. Brown (Ed.), *Biotic communities of the American Southwest-United States and Mexico* (pp. 181–221). Desert Plants 4(1–4).
- Van Asch, T. W. J., van Dijk, S. J. E., & Hendricks, M. R. (2001). The role of overland flow and subsurface flow on the spatial distribution of soil moisture in the topsoil. *Hydrological Processes*, 15, 2325–2340.
- Vincini, M., Reeder, D., & Frazzi, E. (2011). Influences of topography on TM data and vegetation indices of deciduous forests. http://srtm.die.unifi.it/Atticonvegno/doc/RP16.pdf. Accessed 8 March 2011.
- White, J. D., & Running, S. W. (1994). Testing scale-dependent assumptions in regional ecosystem simulations. *Journal of Vegetation Science*, 5, 687–702.
- Witty, J. H., Graham, R. C., Hubbert, K. R., Doolittle, J. A., & Wald, J. A. (2003). Contributions of water supply from the weathered bedrock zone to forest soil quality. *Geoderma*, 114, 389–400.
- Wolff, D. B., Marks, D. A., Amitai, E., Silberstein, D. S., Fisher, B. L., Tokay, A., Wang, J., & Pippitt, J. L. (2005). Ground validation for the tropical rainfall measuring mission (TRMM). *Journal of Atmospheric and Oceanic Technology*, 22, 365–380.
- Zaytsev, O., Cervantes-Duarte, R., Montante, O., & Gallegos-García, A. (2003). Coastal upwelling activity on the Pacific shelf of the Baja California Peninsula. *Journal of Oceanography*, 59, 489–502.
- Zinko, U., Seibert, J., Dynesius, M., & Nilsson, C. (2005). Plant species numbers predicted by a topography based groundwater flow index. *Ecosystems*, 8, 430–441.

